



Rapid Prototyping Journal

Emerald Article: Application of similitude techniques to functional testing of rapid prototypes

Alan J. Dutson, Kristin L. Wood, Joseph J. Beaman, Richard H. Crawford, David L. Bourell

Article information:

To cite this document: Alan J. Dutson, Kristin L. Wood, Joseph J. Beaman, Richard H. Crawford, David L. Bourell, (2003), "Application of similitude techniques to functional testing of rapid prototypes", Rapid Prototyping Journal, Vol. 9 Iss: 1 pp. 6 - 13

Permanent link to this document:

<http://dx.doi.org/10.1108/13552540310455593>

Downloaded on: 22-07-2012

References: This document contains references to 8 other documents

Citations: This document has been cited by 1 other documents

To copy this document: permissions@emeraldinsight.com

This document has been downloaded 1170 times since 2005. *

Users who downloaded this Article also downloaded: *

Yongnian Yan, Rendong Wu, Renji Zhang, Zhuo Xiong, Feng Lin, (2003), "Biomaterial forming research using RP technology", Rapid Prototyping Journal, Vol. 9 Iss: 3 pp. 142 - 149

<http://dx.doi.org/10.1108/13552540310477445>

Suman Das, Scott J. Hollister, Colleen Flanagan, Adebisi Adewunmi, Karlin Bark, Cindy Chen, Krishnan Ramaswamy, Daniel Rose, Erwin Widjaja, (2003), "Freeform fabrication of Nylon-6 tissue engineering scaffolds", Rapid Prototyping Journal, Vol. 9 Iss: 1 pp. 43 - 49

<http://dx.doi.org/10.1108/13552540310455656>

Thomas Himmer, Anja Techel, Steffen Nowotny, Eckhard Beyer, (2003), "Recent developments in metal laminated tooling by multiple laser processing", Rapid Prototyping Journal, Vol. 9 Iss: 1 pp. 24 - 29

<http://dx.doi.org/10.1108/13552540310455629>

Access to this document was granted through an Emerald subscription provided by UNIVERSITY OF TEXAS AUSTIN

For Authors:

If you would like to write for this, or any other Emerald publication, then please use our Emerald for Authors service. Information about how to choose which publication to write for and submission guidelines are available for all. Please visit www.emeraldinsight.com/authors for more information.

About Emerald www.emeraldinsight.com

With over forty years' experience, Emerald Group Publishing is a leading independent publisher of global research with impact in business, society, public policy and education. In total, Emerald publishes over 275 journals and more than 130 book series, as well as an extensive range of online products and services. Emerald is both COUNTER 3 and TRANSFER compliant. The organization is a partner of the Committee on Publication Ethics (COPE) and also works with Portico and the LOCKSS initiative for digital archive preservation.

*Related content and download information correct at time of download.

Application of similitude techniques to functional testing of rapid prototypes

Alan J. Dutson

Kristin L. Wood

Joseph J. Beaman

Richard H. Crawford and

David L. Bourell

The authors

Alan J. Dutson, Kristin L. Wood, Joseph J. Beaman, Richard H. Crawford and David L. Bourell are all based at the Department of Mechanical Engineering, The University of Texas at Austin, Austin, TX, USA.

Keywords

Rapid prototyping, Design

Abstract

Functional testing of rapid prototypes (RP) represents an exciting area of research in solid freeform fabrication. One approach to functional testing is to use similitude techniques to correlate the behavior of an RP model and a product. Previous research at UT, Austin has resulted in the development of an empirical similitude technique for correlating the behavior of parts with different material properties. Advances in the empirical similitude technique are presented in this paper. Sources of coupling between material properties and geometric shape that produce distortions in the current empirical similitude technique are outlined. A modified approach that corrects such distortions is presented. Numerical examples are used to illustrate both the current and the advanced empirical similitude methods.

Electronic access

The research register for this journal is available at <http://www.emeraldinsight.com/researchregisters>

The current issue and full text archive of this journal is available at <http://www.emeraldinsight.com/1355-2546.htm>

1. Introduction

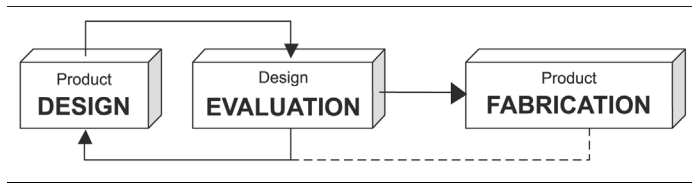
A typical product development process can be abstracted into three broad categories: design, evaluation, and fabrication (Figure 1). The design and evaluation activities are iterated until a satisfactory design (one that meets customer needs) is achieved. If a design is properly evaluated, product fabrication can be carried out without further changes to the design. If, however, a design is not properly evaluated and refined, product fabrication may reveal unexpected product behaviors that can only be corrected through expensive design changes. Since design changes that occur late in the development process are extremely expensive and difficult to implement, it is essential that a design be thoroughly evaluated and refined before fabrication begins.

Prototypes are a powerful and commonly used means of evaluating product designs. Prototypes can either be physical or virtual in nature. Virtual prototypes (VP) include computer models, simulations, virtual reality, etc. Physical prototypes can either be traditional prototypes, which are created through typical manufacturing processes and manual construction, or rapid prototypes (RP), which are created with solid freeform fabrication techniques (Beaman *et al.*, 1997).

Improvements in computer equipment and software tools have produced a trend in many industries toward increased use of VP and decreased use of physical prototypes. Benefits of VP include relatively low costs, quick evaluations of design changes, and effective means of exploring the design space of a product. The trend towards increased use of VP is likely to continue in today's competitive industries where development costs and time to market must continually be reduced.

VP have not entirely replaced physical prototypes in many development processes, however. Physical prototypes continue to fill

The research reported in this document was supported, in part, by NSF grant number DMI-9988880 and ATP grant number 003658-0079-2001. The authors also wish to acknowledge the support of the Cullen Trust for Higher Education Endowed Professorship #1, the Gloyna Regents Chair in Engineering, the Temple Foundation Endowed Faculty Fellowship #3, and the Temple Foundation Endowed Faculty Professorship #2. Any opinions, findings, or recommendations are those of the authors and do not necessarily reflect the views of the sponsors.

Figure 1 Abstraction of product development process

a vital role in many aspects of product development, such as the following.

- Physical prototypes are often better suited for certain types of product evaluations, such as ergonomics, proportions, customer feedback, etc.
- Physical prototypes capture physical phenomena that may be overlooked or are impossible to capture in virtual models. The more complex a system is, the more difficult it becomes to capture all relevant physical phenomena in a virtual model.
- Physical prototypes can provide actual test data against which a virtual model is compared. This activity represents an important aspect of the verification and refinement process for virtual models.

While VP have improved many aspects of the product development process, physical prototypes continue to be an integral element of the process. Solid freeform fabrication, in fact, opens entirely new avenues for physical prototyping that did not exist previously.

The third item in the list above indicates that physical and VP can work as complements to each other in improving the design process. The goal of our research is to improve the way in which physical prototypes are used in verifying and refining virtual models. The specific objective of this research is to reduce the time required to verify virtual models by performing functional testing on RP instead of on traditional prototypes. Performing function testing with RP has the potential to significantly reduce product development cycle times.

Extremely limited functional testing has traditionally been performed with RP since material properties and part sizes that are available from RP technologies are rarely the same as those of the product. In other words, while the form of the RP may be the same as that of the product, the functional behavior is, in general, different. In order to overcome this limitation, similitude techniques are used to correlate the behavior of the prototype with that of the product. The two similitude techniques considered here are the traditional

similitude method (TSM), which is also known as dimensional analysis, and the empirical similitude method (ESM).

2. Background

The TSM is a similitude method that relies solely on dimensional information to correlate the behavior of two similar systems. The ESM, on the other hand, uses empirical data to correlate the behavior of the two systems. Both the TSM and the ESM are reviewed briefly in the following sections.

2.1 Traditional similitude method

The field of dimensional analysis (herein referred to as the TSM) has developed over several centuries. The basic idea of the TSM is to create scale factors, based on the dimensions of system parameters, which are used to correlate the behavior of two similar systems. The first step in the TSM process is to recast the dimensional equation that describes the system into dimensionless form, as follows:

$$g(d_1, d_2, \dots, d_n) = 0 \Rightarrow f(\pi_1, \pi_2, \dots, \pi_N) = 0 \quad (1)$$

where d_j are dimensional parameters, π_i are dimensionless products, and $N < n$. For two similar systems (a product, p, and a model, m) the dimensionless products can be represented as

$$\begin{aligned} f(\pi_{p,1}, \pi_{p,2}, \dots, \pi_{p,N}) &= 0 \\ f(\pi_{m,1}, \pi_{m,2}, \dots, \pi_{m,N}) &= 0 \end{aligned} \quad (2)$$

or, in terms of a particular parameter of interest, say X , as

$$\begin{aligned} \pi_{p,X} &= f(\pi_{p,1}, \pi_{p,2}, \dots, \pi_{p,N-1}) \\ \pi_{m,X} &= f(\pi_{m,1}, \pi_{m,2}, \dots, \pi_{m,N-1}) \end{aligned} \quad (3)$$

For the two corresponding systems described by equation (3), the TSM states that $\pi_{p,X} = \pi_{m,X}$ if $\pi_{p,i} = \pi_{m,i}$ for all $i = 1, 2, \dots, N-1$. Many references exist that contain systematic derivations of dimensionless parameters from sets of dimensional parameters (Barr, 1979; Langhaar, 1951).

Two systems which satisfy the TSM constraints ($\pi_{p,i} = \pi_{m,i}$ for all $i = 1, 2, \dots, N-1$) are said to be well-scaled,

while systems which do not satisfy the constraints are said to be distorted. Many sources of system distortion exist which produce errors in the TSM approach (this type of distortion is referred to as model distortion). If, for example, one of the dimensionless products contains a parameter that is constant in the model system but variable in the product system, then the system becomes distorted and the TSM yields inaccurate results.

2.2 Empirical similitude method

The ESM provides a means of correlating distorted systems. The fundamental concept of the ESM is shown in Figure 2. Unlike the traditional method, which relies solely on dimensional information for correlating systems, the ESM is able to correlate distorted systems by utilizing empirical data from a simplified specimen pair. The model specimen (MS) is a geometrically simplified version of the model, while the product specimen (PS) is a geometrically simplified version of the product. The ESM uses measured values from the MS, the PS, and the model to predict the behavior of the product. The basic assumptions of the ESM are as follows (Wood, 2002).

- (1) The model and the MS can be tested to determine the state variation caused by changes in geometric shape, or form. A form transformation matrix \mathbf{F} can be created which represents the variation in the state vector \mathbf{x} caused by the change in geometric shape.
- (2) The MS and the PS can be tested to determine the state variation caused by changes in material properties, size, and loading conditions (all of the parameters

that are typically scaled between a product and a model). A scale transformation matrix \mathbf{S} can be created which represents the variation in the state vector \mathbf{x} caused by changes in size, material properties, and loading conditions, independent of geometric shape.

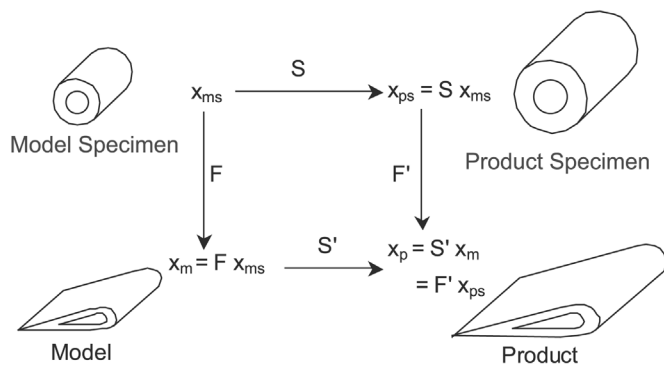
The state of the product can be predicted by multiplying the state of the model by \mathbf{S}' or by multiplying the state of the PS by \mathbf{F}' as shown in Figure 2. A basic assumption of the ESM is that $\mathbf{S} = \mathbf{S}'$ and $\mathbf{F} = \mathbf{F}'$ or that \mathbf{S} and \mathbf{F} are independent.

Figure 3 shows qualitatively the application of ESM with respect to the TSM and full-scale testing. We claim that the ESM is a more accurate approach, in general, than the TSM. We also claim that the ESM is a better approach for correlating complex systems whose governing parameters may not be well known, as required by the TSM. However, the range of application of the ESM, as represented by the boundary lines in Figure 3, has not yet been clearly established. An evaluation of the current ESM boundaries, as well as a means to extend those boundaries, is presented below.

3. Range of application of the ESM

The ESM theory is valid as long as $\mathbf{S} = \mathbf{S}'$ and $\mathbf{F} = \mathbf{F}'$ as shown in Figure 2. Conditions that can cause $\mathbf{S} \neq \mathbf{S}'$ and $\mathbf{F} \neq \mathbf{F}'$, which are termed specimen distortions, are summarized in Figure 4. If the ESM is set up with consistent scaling and with consistent material properties in the model and product families, the only source of specimen

Figure 2 Empirical similarity method. Adapted from Cho *et al.*, 1999



Source: Adapted from Cho (1999)

Figure 3 TSM vs ESM

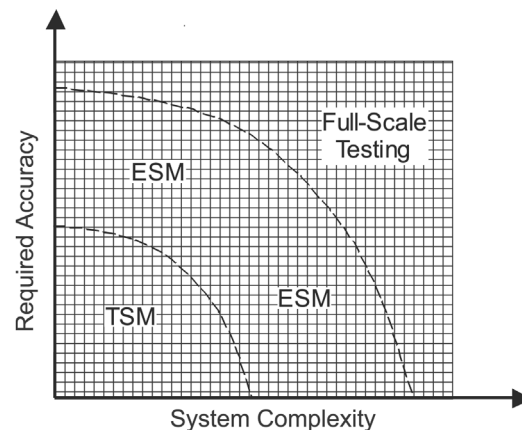
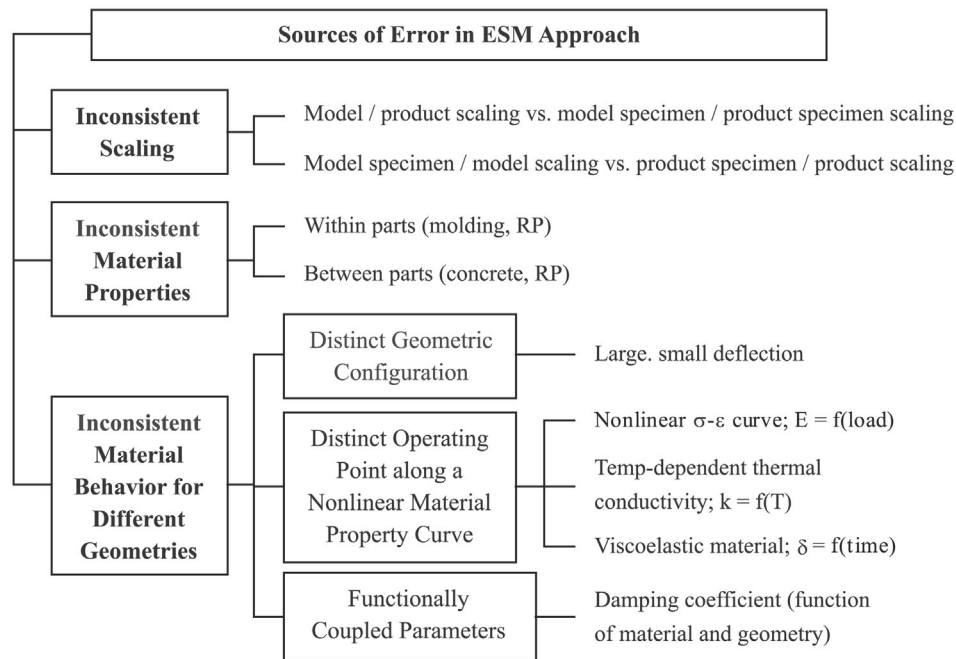


Figure 4 Sources of error in the ESM

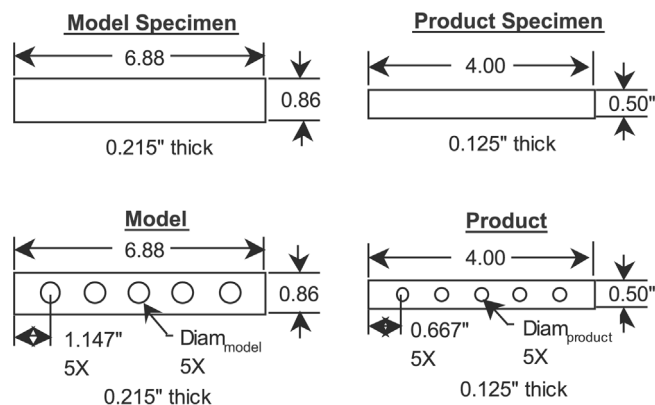
distortion comes from inconsistent material behavior in the model or product family. It is important to notice the distinction that is made between material properties and material behavior: material properties refer to the global properties of the material, and material behavior refers to the response of the material under specific loading and boundary conditions. For example, a stress-softening material behaves differently – either “flexibly” or “stiffly” – depending on its specific operating point along the non-linear stress-strain curve.

The ESM error that results from inconsistent material behavior is perhaps more subtle and difficult to anticipate than the other classes of specimen distortion. Three finite element studies are used to illustrate this type of specimen distortion. Each study illustrates one of the three subclasses of material behavior distortion and are listed in Figure 4. Each study also involves a particular type of model distortion (otherwise the TSM would be used rather than the ESM). The model distortions reflect conditions that are typical with RP, namely non-linear material behavior, limitations in size, and non-isotropic material structures. The product to be evaluated is a cantilever beam with five holes along the length. The deflection of the beam under a concentrated load at the tip is the system behavior of interest.

The ESM setup for the three finite element studies is shown in Figure 5. In each study, three different hole diameters are considered for the product beam (small holes with 0.15 in. diameter, medium holes with 0.25 in. diameter, and large holes with 0.35 in. diameter). Each beam is modeled with linear shell elements (S4R elements) using ABAQUS™ software. Large deflection effects are considered in each study. Beam deflection is monitored and recorded at ten equally spaced load increments.

3.1 ESM study 1: linear vs non-linear material properties

The first ESM study involves a linear stress-strain curve for the product family and a non-linear stress-strain curve for the model

Figure 5 ESM setup for finite element studies

family. The constant value of Young’s modulus for the product family is 10,150 ksi (equal to that of aluminum). The variable value of Young’s modulus for the model family is defined with a Ramberg-Osgood curve, which is described by the following equation (ABAQUS, 2001):

$$\epsilon = \frac{\sigma}{E} \left(1 + \alpha \left(\frac{\sigma}{\sigma^0} \right)^{n-1} \right) \quad (4)$$

where σ = stress, ϵ = strain, E = Young’s modulus (defined as the slope of the stress-strain curve at zero stress), α = “yield” offset, σ^0 = yield stress, and n =hardening exponent for the “plastic” (non-linear) term. By using different parameter values in equation (4), three different sets of material properties with increasing degrees of non-linearity are defined (Table I). Evaluating three geometric cases for each of the three different material properties gives a total of nine cases for this study. In each case, the ESM prediction of beam deflection is compared to the actual beam deflection, and a percent error in the ESM prediction is calculated. A plot of the results is shown in Figure 6. The model distortion, which is plotted along the abscissa in Figure 6 and is included in Table I, is calculated as the residual

sum of squares between the non-linear and linear stress-strain curves, as follows:

$$SS(\text{residual}) = \sum_{i=1}^n (\epsilon_{nl} - \epsilon_l)^2 \quad (5)$$

where ϵ_{nl} and ϵ_l are non-linear and linear values of strain, respectively, at every 10 psi increment of stress (equation (4)); DeVor *et al.*, 1992). The error at zero model distortion, which corresponds to a well-scaled system, is assumed to be zero.

This source of ESM error is clarified by plotting the maximum operating stress in the (non-linear) model material for the various geometric shapes. Figure 7 contains such a plot for material 2. Because the model material has a non-linear stress-strain curve, while the product material has a linear stress-strain curve, a change in geometric shape produces a different effect in the model family than it does in the product family. As the holes in the beam increase in diameter, the maximum stress (which occurs at the stress concentration around the first hole) increases. As the maximum stress increases, the model material behaves in a more flexible manner (i.e. the effective value of Young’s modulus decreases) while the behavior of the product material remains the same (with a constant value of Young’s modulus). Since the material behavior is dependent on geometric shape, the ESM assumption is violated and errors result. The specimen distortion illustrated in this example falls under the category of

Table I Material properties for ESM study 1

Material	E (ksi)	α	σ^0 (ksi)	n	Distortion
1	150	0.40	3	2.0	0.52
2	320	0.43	3	3.0	0.67
3	500	2.00	3	2.5	2.60

Figure 6 Results for ESM study 1

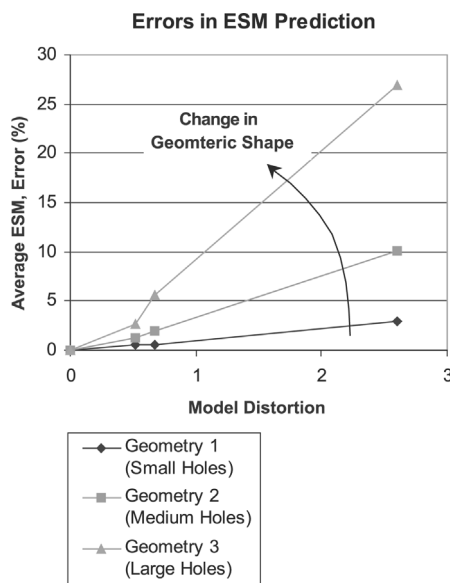
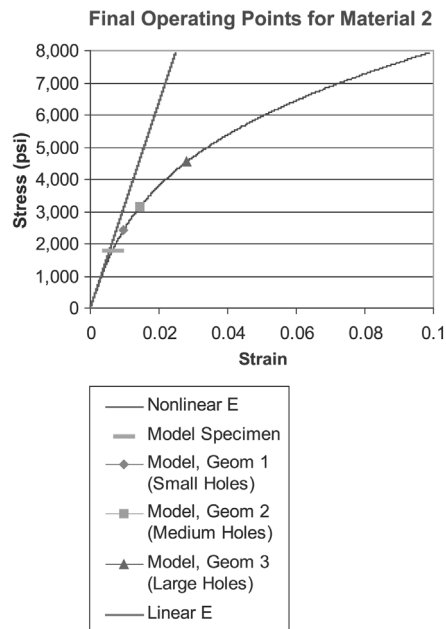


Figure 7 Maximum stress for various geometries



“distinct operating point along a non-linear material property curve” in Figure 4.

3.2 ESM study 2: distortion in size

The second ESM study investigates the effect of distorting the length of the model and the MS. All of the other beam parameters are well scaled. The five beam lengths that are considered are shown in Table II. The degree of model distortion is defined as

$$\text{distort}_L = \frac{L_i - L_{WS}}{L_{WS}} * 100, \quad i = 1, 2, 3, 4, 5 \quad (6)$$

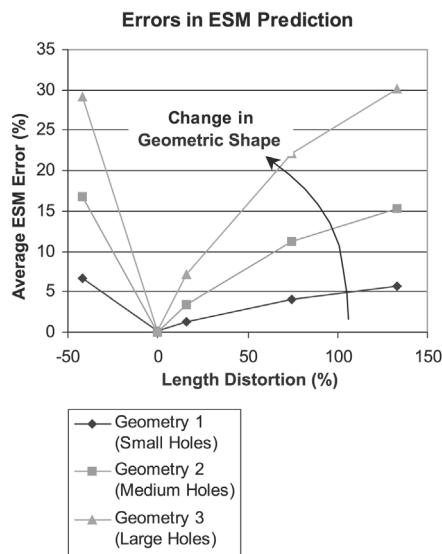
where distort_L is the amount of distortion in length, L_i is the length of each beam, and L_{WS} is the length of the well-scaled beam. Note that case 2 in Table II corresponds to a well-scaled system, and we would expect no error in either the TSM or the ESM results. Case 1 in Table II represents a model beam that is “too short,” and cases 3-5 represent model beams that are “too long.”

The results of the study are shown in Figure 8. The ESM error is caused by the fact that the length distortion in the model family produces a different geometric configuration in the model family than in the product family. Because of large deflection effects, a change in

Table II Setup for ESM study 2

Case	Length (in.)	Model distortion (%)
1	4.00	-41.9
2	6.88	0.00
3	8.00	16.3
4	12.0	74.4
5	16.0	133.0

Figure 8 Results for ESM study 2



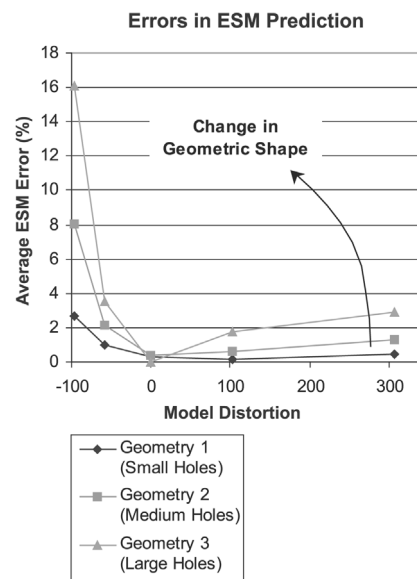
the geometric shape of the product has a different effect on beam deflection than a corresponding change in the geometric shape of the (already highly deflected) model. The specimen distortion illustrated in this example falls under the category of “distinct geometric configuration” in Figure 4.

3.3 ESM study 3: distinct material structures

The final ESM study involves distinct material structures between the product family and the model family. Specifically, the product family exhibits isotropic material properties, while the model family exhibits a form of orthotropy known as *transverse isotropy*. A material that has a transverse isotropic structure has a plane of isotropy at every point in the material (ABAQUS, 2001). Several distorted values of out-of-plane shear modulus (out of the page in Figure 5) are considered in the study. The degree of model distortion is calculated by replacing the length parameters in equation (6) with out-of-plane shear modulus parameters.

The results of the ESM study 3 are shown in Figure 9. The ESM error comes from the fact that total beam deflection is the sum of the deflection due to normal stresses and deflection due to shear stresses. Since the deflection due to shear stresses varies with shear modulus, the contribution of deflection due to shear becomes different in the model family than in the product family as the value of shear modulus deviates from its well-scaled value. Since total beam deflection is

Figure 9 Results for ESM study 3



inherently a function of material properties and geometric shape, this study illustrates the type of specimen distortion classified under “functionally coupled parameters” in Figure 4.

4. Modified ESM approach

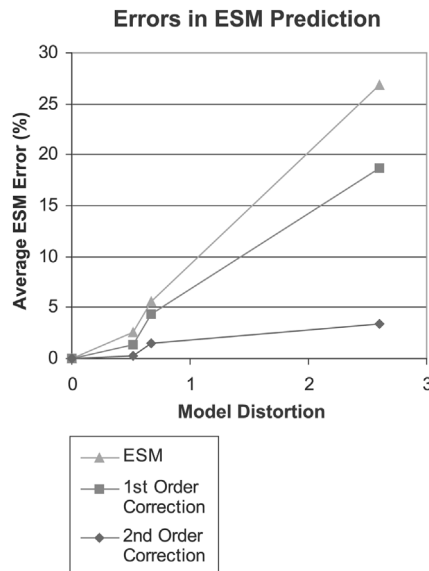
The three studies presented earlier illustrate situations in which the ESM assumptions are no longer valid and $\mathbf{S} \neq \mathbf{S}'$ and $\mathbf{F} \neq \mathbf{F}'$. The modified ESM approach captures the change in the \mathbf{S} transformation matrix as the geometric shape changes by utilizing one or more intermediate specimen pairs (Figure 10). By quantifying the change in \mathbf{S} with respect to the change in hole diameter, a Lagrange interpolating polynomial is constructed to predict \mathbf{S}' (Burden and Faires, 1989). Of course, the more intermediate specimen pairs that are used, the higher the degree of the interpolating polynomial and the higher the prediction accuracy of \mathbf{S}' .

Let us now consider the beam with large holes as the product beam, and the beams with small holes and medium holes as intermediate specimen pairs. With two intermediate specimen pairs, both 1st order and 2nd order polynomials can be constructed to estimate the transformation matrix between the product and the model beams. Figure 11 shows the reduction in ESM prediction error that results from using both 1st order and 2nd order polynomials. Similar improvements in prediction accuracy are also realized in studies 2 and 3.

5. Conclusions

The ESM has shown significant improvements over the TSM in predicting product performance when distortions

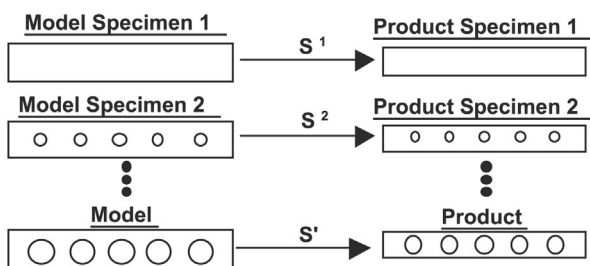
Figure 11 Modified ESM results for study 1



between a product and a model exist. While the ESM typically produces highly accurate results, several sources of specimen distortion that cause the ESM assumptions to become invalid have been identified. The studies presented in this paper illustrate the ESM prediction errors that result from various types of specimen distortion. A modified ESM approach, which uses intermediate specimen pairs to capture the change in the transformation matrix with changes in geometric shape, has been shown to improve ESM predictions.

Further areas of research include expanding the results presented here into other areas, such as heat transfer applications. In addition, further research is needed to be able to quantify the change in the transformation matrix when the geometry change involves different geometric shapes (e.g. circular holes vs triangular holes). Finally, an overall approach for functional testing with RP is needed which indicates which method (TSM, ESM, advanced ESM, or full scale testing) is appropriate in different situations.

Figure 10 Modified ESM approach



References

- ABAQUS (2001), Hibbitt, Karlsson and Sorensen, Inc.: *Standard User's Manual*, version 6.2.
- Barr, D.I.H. (1979), "Echelon matrices in dimensional analysis", *International Journal of Mechanical Engineering Education*, Vol. 7 No. 2, pp. 85-9.
- Beaman, J.J., Barlow, J.W., Bourell, D.L., Crawford, R.H., Marcus, H.L. and McAlea, K.P. (1997), *Solid Freeform*

- Fabrication: A New Direction in Manufacturing*, Kluwer, Massachusetts.
- Burden, R.L. and Faires, J.D. (1989), *Numerical Analysis*, PWS Kent, Boston.
- Cho, U., Wood, K.L. and Crawford, R.H. (1999), "System-level functional testing for scaled prototypes with configurational distortions," *Proceedings of the 1999 ASME DETC*, Las Vegas, NV.
- DeVor, R.E., Chang, T. and Sutherland, J.W. (1992), *Statistical Quality Design and Control*, Macmillan, New York.
- Langhaar, H.L. (1951), *Dimensional Analysis and Theory of Models*, John Wiley and Sons, New York.
- Wood, J.J. (2002), "Design methodology using empirical and virtual analysis with application to compliant systems", Doctoral dissertation, Colorado State University.